Science in China Ser. G Physics and Astronomy 2004 Vol.47 No.1 8—16

Imaging theory of nonlinear second harmonic and third harmonic generations in confocal microscopy

TANG Zhilie[1], XING Da[2] & LIU Songhao[2]

1. Department of Physics, South China Normal University, Guangzhou 510631, China;
2. School for Information and Optoelectronic Science and Engineering, South China Normal University, Guangzhou 510631, China

Correspondence should be addressed to Tang Zhilie (email: tangzhl@scnu.edu.cn)

Received April 23, 2003

Abstract The imaging theory of nonlinear second harmonic generation (SHG) and third harmonic generation (THG) in confocal microscopy is presented in this paper. The nonlinear effect of SHG and THG on the imaging properties of confocal microscopy has been analyzed in detail by the imaging theory. It is proved that the imaging process of SHG and THG in confocal microscopy, which is different from conventional coherent imaging or incoherent imaging, can be divided into two different processes of coherent imaging. The three-dimensional point spread functions (3D-PSF) of SHG and THG confocal microscopy are derived based on the nonlinear principles of SHG and THG. The imaging properties of SHG and THG confocal microscopy are discussed in detail according to its 3D-PSF. It is shown that the resolution of SHG and THG confocal microscopy is higher than that of single- and two-photon confocal microscopy.

Keywords: second harmonic generation, third harmonic generation, confocal microscopy, three-dimensional point spread function.

DOI: 10.1360/03yw0023

It is reported recently that nonlinear optical phenomenon of SHG and THG has been observed in many biological tissues[1—6]. SHG and THG have been used to perform the three-dimensional imaging in living tissues and have attracted much attention recently. There are many advantages of using SHG and THG to perform the three-dimensional imaging in living tissues, such as noninvasive and no photobleaching, in addition to the imaging properties of multi-photon fluorescence imaging[7−9]. Firstly, unlike in the single- and multi-photon fluorescence processes, only virtual states are involved in harmonic generation that result in no energy deposition and thus no photodamage or bleaching is expected. Secondly, SHG or THG imaging needs no fluorescent labels and brings no photobleaching or toxicity. Thus, SHG or THG imaging is an idea tool for living cell tomography or three-dimensional imaging. Since SHG does

not occur in optically isotropic media, SHG microscopy was demonstrated in the studies of SHG crystals and was then applied to biological study, including the study of membrane potentials tissue polarity. THG microscopy was applied to transparent objects, and effective THG occurred only in interfaces optical inhomogeneity. With a cubic dependence, the THG process provides even better intrinsic sectioning resolution than SHG with the same excitation laser wavelength. In theoretical study, the imaging principles of two-photon or multi-photon confocal microscopy have been discussed extensively by many authors[10—12], however, the imaging properties of SHG and THG are very different from that of two-photon or multi-photon imaging because of the difference of their coherence and their generation process. For SHG and THG imaging, because SHG and THG are coherent, their imaging process can be divided into two coherent imaging processes. But two- or multi-photon fluorescence is incoherent, their imaging process is incoherent imaging. In addition, SHG and THG imaging is based on the spatial distribution of the second-order and the third-order nonlinear susceptibility ($c^{(2)}(2w)$ and $c^{(3)}(2w)$) of materials. While two- or multi-photon imaging is based on the spatial distribution of two- or multi-photon absorption coefficient of material. Therefor, the imaging theory of two- or multi-photon confocal microscopy cannot be used to describe the imaging property of SHG and THG confocal microscopy. It is necessary to derive the imaging theory of SHG and THG confocal microscopy.

1 3D-PSF of SHG and THG confocal microscopy

The diagram of SHG and THG confocal microscopy is shown in fig. 1. A laser beam from a point source is focused to objective plan O by an objective L_1 and induces SHG and THG. The SHG and THG are collected by a collecting lens L_2, filtered by a filter F and detected by a detector D. According to Fourier imaging theory[13], imaging properties of an imaging system can be described completely by its 3D-PSF. So, we must derive the 3D-PSF of SHG and THG confocal microscopy firstly. Accounting for the nonlinear effect of SHG and THG, the imaging process of SHG and THG is much more complex than that of conventional linear imaging. Because the complex amplitudes of SHG and THG are proportional to the square and cube of the complex amplitude of excitation light, respectively, therefore, the imaging processes of SHG and THG are neither conventional coherent imaging where the complex amplitude of image is proportional to that of excitation light, nor incoherent imaging where the intensity of image is proportional to that of excitation light. What is more important is that SHG and THG only occurred when the power density of excitation light reaches a threshold. Thus, only within a small focal area where the power density of excitation light reaches a threshold can we generate SHG and THG. Outside this area, the intensity of excitation light decreased sharply and cannot

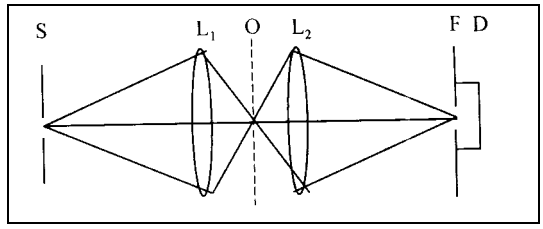

Fig. 1. Diagram of SHG and THG confocal microscopy.

reach the threshold, thus cannot generate SHG and THG. It means that the focal spot of SHG and THG is smaller than that of the excitation light. In other words, the nonlinear effect of SHG and THG can sharpen their focal spot themselves. It is interesting that this sharpening process is caused by the nonlinear effect of SHG and THG rather than objective lens. Obviously, this sharpening process cannot be described by the conventional 3D-PSF of objective lens. It is necessary to derive a new 3D-PSF including the nonlinear effect of SHG and THG.

Generally, the light source function and the detector function are assumed as plane function and described by the following function, respectively:

$$S(u_{\mathrm{s}}) = S(u_{\mathrm{sx}}, u_{\mathrm{sy}}; u_{\mathrm{s}}) = S_1(u_{\mathrm{sx}}, u_{\mathrm{sy}})d(u_{\mathrm{s}}), \quad S_1(u_{sx}, u_{sy}) = \begin{cases} 1, & u_{\mathrm{sx}}^2 + u_{\mathrm{sy}}^2 \le R_{\mathrm{s}}^2 \\ 0, & \text{others} \end{cases}, \tag{1}$$

$$D(u_{\mathrm{d}}) = D(u_{\mathrm{dx}}, u_{\mathrm{dy}}; u_{\mathrm{d}}) = D_1(u_{\mathrm{dx}}, u_{\mathrm{dy}})d(u_{\mathrm{d}}), \quad D_1(u_{\mathrm{sx}}, u_{\mathrm{sy}}) = \begin{cases} 1, & u_{\mathrm{dx}}^2 + u_{\mathrm{dy}}^2 \le R_{\mathrm{d}}^2 \\ 0, & \text{others} \end{cases}, \tag{2}$$

where, R_{s} and R_{d} are the radii of the source and the detector, respectively (in terms of the optical coordinate). The optical coordinate vectors on different planes of source, objective and detector are described by $u_{\mathrm{s}}(u_{\mathrm{sx}}, u_{\mathrm{sy}}; u_{\mathrm{s}})$, $u_o(u_{ox}, u_{oy}; u_o)$, $u_{\mathrm{d}}(u_{\mathrm{dx}}, u_{\mathrm{dy}}; u_{\mathrm{d}})$, and the optical coordinate vectors of SHG and THG on objective planes are $u'_o(u'_{ox}, u'_{oy}; u'_o)$ and $u''_o(u''_{ox}, u''_{oy}; u''_o)$, respectively. Considering that the wavelength of excitation light is twice and triple that of SHG and THG, respectively, the optical coordinate vectors of excitation light, SHG and THG are as follows:

$$\begin{aligned}
&u_{ox} = \frac{2p}{l_1} x_o \sin a, \quad u_{oy} = \frac{2p}{l_1} y_o \sin a; \quad u_o = \frac{2p}{l_1} z_o \sin^2 a, \\
&u'_{ox} = \frac{2p}{l_2} x_o \sin a = \frac{4p}{l_1} x_o \sin a = 2u_{ox}, \quad u'_{oy} = \frac{2p}{l_2} y_o \sin a = \frac{4p}{l_1} y_o \sin a = 2u_{oy}, \\
&u'_o = \frac{2p}{l_2} z_o \sin^2 a = \frac{4p}{l_1} z_o \sin^2 a = 2u_o, \\
&u''_{ox} = \frac{2p}{l_3} x_o \sin a = \frac{6p}{l_1} x_o \sin a = 3u_{ox}, \quad u''_{\mathrm{dy}} = \frac{2p}{l_3} y_o \sin a = \frac{6p}{l_1} y_o \sin a = 3u_{oy}, \\
&u''_o = \frac{2p}{l_3} z_o \sin^2 a = \frac{6p}{l_1} z_o \sin^2 a = 3u_o,
\end{aligned} \tag{3}$$

where $\sin a$ is the numerical aperture of the objective lens, l_1, l_2, l_3 are the wavelengths of excitation, SHG and THG, respectively. (x_o, y_o, z_o) are the Descartes coordinates on the objective plane.

In fact, the complex imaging processes of SHG, THG confocal microscopy can be divided into two simpler processes, and each imaging process can be described by

coherent imaging or incoherent imaging. The first imaging process is that a point source S are focused to object O by objective lens L_1 and induces SHG and THG. The second imaging process is that SHG and THG generated from the object O are focused to the detector by a collecting lens L_2. According to Fourier imaging theory, the imaging process from light source to the object plane is a coherent imaging process. So the complex amplitude distribution of excitation light on the object plane is

$$U_1(u_o) = \iiint_{\infty} S(u_s) h_1(u_o - u_s) du_s, \tag{4}$$

where $h_1(u_o - u_s)$ is three-dimensional amplitude point spread function of the objective lens. According to the principles of nonlinear optics[14], the complex amplitude of SHG is proportional to the square of the complex amplitude of excitation light. Thus, the complex amplitude of SHG is

$$U_2(u_p - u_o') = \left| \iiint_{\infty} S(u_s) h_1(u_o - u_s) du_s \right|^2 \cdot O(u_p - u_o'), \tag{5}$$

where $O(u_p - u_o')$ represents the spatial distribution of SHG, which is proportional to the second order nonlinear susceptibility $c^{(2)}(2w)$ of the material. u_p is the position vectors of scanning point. It is obvious that SHG imaging is used to obtain the image of spatial distribution of the second order nonlinear susceptibility $c^{(2)}(2w)$ of material.

The second process of SHG imaging, from the object plane to the detector plane, is also a coherent imaging process because of coherence of SHG, thus the complex amplitude distribution of SHG on the detector plane can be expressed as

$$U_3(u_d, u_p) = \iiint_{\infty} \left[\left| \iiint_{\infty} S(u_s) h_1(u_o - u_s) du_s \right|^2 \cdot O(u_p - u_o') \right] \cdot h_2(u_d - u_o') du_o', \tag{6}$$

where $h_2(u_d - u_o')$ is three-dimensional amplitude point spread function of collecting lens L_2. It is obvious that the second imaging process of SHG confocal microscopy is different from that of two-photon confocal microscopy where the imaging process is incoherent imaging because of the incoherence of two-photon fluorescence.

Considering that the detector has a definit aperture $D(u_d)$, the complex amplitude distribution of SHG on the detector surface can be expressed as:

$$\begin{aligned} U_4(u_p) &= \iiint_{\infty} \left\{ \iiint_{\infty} \left[\left| \iiint_{\infty} S(u_s) h_1(u_o - u_s) du_s \right|^2 \cdot O(u_p - u_o') \right] \cdot h_2(u_d - u_o') du_o' \right\} \cdot D(u_d) du_d \\ &= \iiint_{\infty} \left\{ \left| \iiint_{\infty} S(u_s) h_1(u_o - u_s) du_s \right|^2 \cdot \iiint_{\infty} h_2(u_o' - u_d) D(u_d) du_d \right\} O(u_p - u_o') du_o' \\ &= \{ | S(u_o) \otimes_3 h_1(u_o) |^2 \cdot [h_2(u_o') \otimes_3 D(u_d)] \} \otimes_3 O(u_p). \end{aligned} \tag{7}$$

According to the imaging theory, in a coherent imaging system, the complex amplitude distribution of image is equal to convolution of the complex amplitude distribution of object and the point spread function of the imaging system, therefore, the three-dimensional point spread function of SHG imaging system shown in fig. 1 is

$$F_{\mathrm{SHG}}(u)=\{[|S(u_o)\otimes_3 h_1(u_o)|^2]\cdot[h_2(u_o')\otimes_3 D(u_{\mathrm{d}})]\}$$

$$=\{[|S(u_o)\otimes_3 h_1(u_o)|^2]\cdot[h_2(2u_o)\otimes_3 D(u_{\mathrm{d}})]\}. \tag{8}$$

Eq. (8) is the three-dimensional point spread function of SHG confocal microscopy in the condition of off-confocal, because the light source and detector have a definit aperture $S(u_{\mathrm{s}})$ and $D(u_{\mathrm{d}})$, respectively.

As for THG imaging, the complex amplitude of THG is proportional to the cube of the complex amplitude of excitation light. And the wavelength of THG is one-third that of excitation light. The optical coordinate of THG is triple that of excitation light. Thus, the 3D-PSF of THG imaging system can be expressed as:

$$F_{\mathrm{THG}}(u)=\{[|S(u_o)\otimes_3 h_1(u_o)|^3]\cdot[h_2(u_o'')\otimes_3 D(u_{\mathrm{d}})]\}$$

$$=\{[|S(u_o)\otimes_3 h_1(u_o)|^3]\cdot[h_2(3u_o)\otimes_3 D(u_{\mathrm{d}})]\}. \tag{9}$$

For confocal microscopy, the light source and detector are point source and point detector, respectively, $S(u_{\mathrm{s}})=d(u_{\mathrm{s}})$, $D(u_{\mathrm{d}})=d(u_{\mathrm{d}})$. Thus, the 3D-PSF of SHG and THG confocal microscopy can be derived from eqs. (8) and (9) as follows:

$$F_{\mathrm{SHG}}^{\mathrm{con}}(u)=|h_1(u_o)|^2\cdot h_2(u_o)=\left|\iint_{\infty}P_1(x,h)\exp\left[-\frac{ju}{2}(x^2+h^2)\right]\exp[-j(u_x x+u_y h)]dx\,dh\right|^2$$

$$\cdot\iint P_2(x,h)\exp[-ju(x^2+h^2)]\exp[-j(2u_x x+2u_y h)]dx\,dh, \tag{10}$$

$$F_{\mathrm{THG}}^{\mathrm{con}}(u)=|h_1(u_o)|^3\cdot h_2(u_o'')=\left|\iint_{\infty}P_1(x,h)\exp\left[-\frac{ju}{2}(x^2+h^2)\right]\exp[-j(u_x x+u_y h)]dx\,dh\right|^3$$

$$\cdot\iint P_2(x,h)\exp\left[-\frac{j3u}{2}(x^2+h^2)\right]\exp[-j(3u_x x+3u_y h)]dx\,dh, \tag{11}$$

where $P_1(x,h)$ and $P_2(x,h)$ are the aperture function of objective L_1 and collecting lens L_2, respectively.

From eqs. (10) and (11), it is obvious that the 3D-PSF of SHG and THG confocal microscopy is very different from that of two- and three-photon confocal microscopy[10,12]. The cause is as follows. Firstly, the imaging processes of SHG and THG in a confocal microscope belong to twice coherent imaging process, due to the

coherence of SHG and THG. But the imaging processes of two- and three-photon confocal microscopy are two different imaging processes, the first process is coherent imaging and the second process is incoherent imaging, due to the incoherence of two- and three-photon fluorescence. Secondly, the wavelength of SHG and THG is not equal to that of two- and three-photon fluorescence, respectively. Because the wavelength of two- and three-photon fluorescence exists red-shift. Finally, SHG and THG images respond to the spatial distribution of the second-order and the third-order nonlinear susceptibility of material, $c^{(2)}(2w)$ and $c^{(3)}(2w)$, respectively. But two- and three-photon fluorescence images respond to the spatial distribution of two- and three-photon absorption coefficient of material. Because the nonlinear susceptibility and multi-photon absorption coefficient are different physical quantities, their images respond to different structures of material. Especially in centrosymmetric material, we cannot obtain its SHG image due to the second-order nonlinear susceptibility $c^{(2)}(2w) = 0$, but we can obtain its two-photon fluorescence image. In summary, SHG and THG imaging can obtain different images from multi-photon fluorescence image.

2 The 3D imaging properties of SHG and THG confocal microscopy

2.1 The 2D imaging properties and lateral resolution

The 2D imaging properties and lateral resolution of SHG and THG confocal microscopy can be derived from eqs. (10) and (11). Let the axial coordinate $u = 0$ in eq. (10), the amplitude 2D-PSF and intensity 2D-PSF of SHG confocal microscopy can respectively be written as

$$F_{\mathrm{SHG}}^{\mathrm{con}}(u_x,u_y,0)=\left[\frac{2J_1(\sqrt{u_x^2+u_y^2})}{\sqrt{u_x^2+u_y^2}}\right]^2\cdot\left[\frac{2J_1(\sqrt{4u_x^2+4u_y^2})}{\sqrt{4u_x^2+4u_y^2}}\right], \tag{12}$$

$$I_{\mathrm{SHG}}^{\mathrm{con}}(u_x,u_y,0)=\left[\frac{2J_1(\sqrt{u_x^2+u_y^2})}{\sqrt{u_x^2+u_y^2}}\right]^4\cdot\left[\frac{2J_1(\sqrt{4u_x^2+4u_y^2})}{\sqrt{4u_x^2+4u_y^2}}\right]^2, \tag{13}$$

where J_1 is the first order Bessel function. Let the axial coordinate $u = 0$ in eq. (11), the amplitude 2D-PSF and intensity 2D-PSF of THG confocal microscopy can respectively be written as

$$F_{\mathrm{THG}}^{\mathrm{con}}(u_x,u_y,0)=\left[\frac{2J_1(\sqrt{u_x^2+u_y^2})}{\sqrt{u_x^2+u_y^2}}\right]^3\cdot\left[\frac{2J_1(\sqrt{9u_x^2+9u_y^2})}{\sqrt{9u_x^2+9u_y^2}}\right], \tag{14}$$

$$I_{\mathrm{THG}}^{\mathrm{con}}(u_x,u_y,0)=\left[\frac{2J_1(\sqrt{u_x^2+u_y^2})}{\sqrt{u_x^2+u_y^2}}\right]^6\cdot\left[\frac{2J_1(\sqrt{9u_x^2+9u_y^2})}{\sqrt{9u_x^2+9u_y^2}}\right]^2. \tag{15}$$

The numerical plots of eqs. (13) and (15) are displayed in fig. 2(a). To compare with single- and two-photon confocal microscopy and conventional microscopy, the 2D-PSFs of single-photon, two-photon confocal microscopy and conventional microscopy are displayed on the same figure. From fig. 2, we can draw the conclusions as follows:

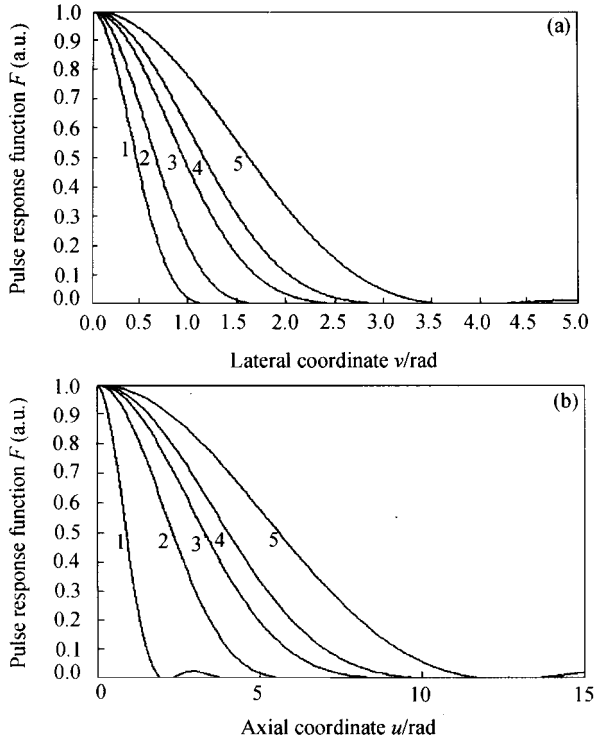

Fig. 2. The lateral PSF (a) and axial PSF (b). 1, THG; 2, SHG; 3, two-photon; 4, single-photon; 5, conventional microscopy.

(i) The lateral resolution of two-photon confocal microscopy is higher than that of single-photon confocal microscopy. Because the nonlinear effect of two-photon transition can sharpen the focal spot of two-photon fluorescence[12].

(ii) The lateral resolution of SHG confocal microscopy is higher than that of two-photon confocal microscopy. Although both SHG and two-photon transition are second order nonlinear process, the wavelength of SHG is shorter than that of two-photon fluorescence, which is due to the red-shift of two-photon fluorescence. It is obvious that the shorter the wavelength, the higher the resolution.

(iii) The lateral resolution of THG confocal microscopy is higher than that of SHG confocal microscopy. Because the nonlinear order of THG is higher than that of SHG. It is obvious that the higher the nonlinear order, the higher the resolution.

(iv) Both SHG and THG confocal microscopes have broken through the resolution limit of Rayleigh's criterion. Because the nonlinear effect of SHG and THG can sharpen

its focal spot, which causes the focal spot of SHG and THG to be smaller than that of excitation light. The smaller the focal spot, the higher the resolution.

2.2 The property of tomography and depth resolution

The unique advantage of a confocal microscope is its high depth resolution and its tomography ability. It is shown that SHG and THG confocal microscopes have higher depth resolution than conventional confocal microscope. Let the lateral coordinate $u_x = 0$, $u_y = 0$ in eq. (10), we can obtain the axial amplitude PSF of SHG confocal microscopy as follows:

$$F_{\mathrm{SHG}}^{\mathrm{con}}(0,0;u)=\left[\frac{\sin(u/4)}{u/4}\right]^2\left[\frac{\sin(u/2)}{u/2}\right]. \tag{16}$$

And axial intensity PSF of SHG confocal microscopy is

$$I_{\mathrm{SHG}}^{\mathrm{con}}(0,0;u)=\left[\frac{\sin(u/4)}{u/4}\right]^4\left[\frac{\sin(u/2)}{u/2}\right]^2. \tag{17}$$

Let the lateral coordinate $u_x = 0$, $u_y = 0$ in eq. (11), we can obtain the axial amplitude PSF of THG confocal microscopy as follows:

$$F_{\mathrm{THG}}^{\mathrm{con}}(0,0;u)=\left[\frac{\sin(u/4)}{u/4}\right]^3\left[\frac{\sin(3u/2)}{3u/2}\right]. \tag{18}$$

And the axial intensity PSF of THG confocal microscopy is

$$I_{\mathrm{THG}}^{\mathrm{con}}(0,0;u)=\left[\frac{\sin(u/4)}{u/4}\right]^6\left[\frac{\sin(3u/2)}{3u/2}\right]^2. \tag{19}$$

The numerical plots of eqs. (17) and (19) are displayed in fig. 2(b). From fig. 2(b), one can see that two-photon confocal microscopy has higher depth resolution than single-photon confocal microscopy, SHG confocal microscopy has higher depth resolution than two-photon confocal microscopy, and THG confocal microscopy has higher depth resolution than SHG confocal microscopy.

3 Conclusion

The imaging theory of SHG and THG confocal microscopy is presented. The nonlinear effect of SHG and THG on the imaging properties of confocal microscopy has been discussed in detail using the imaging theory. From the imaging theory, we can draw the following conclusions:

(1) The imaging processes of SHG and THG confocal microscopy are neither conventional coherent imaging, nor conventional incoherent imaging. It is twice coherent imaging process. Thus it has different 3D-PSF and imaging property from multi-photon confocal microscopy.

(2) The imaging information of SHG and THG is different from that of multi-photon fluorescence, according to the imaging physical quantity. SHG and THG images respond to the spatial distribution of the second-order and the third-order nonlinear susceptibility, $c^{(2)}(2w)$ and $c^{(3)}(2w)$, respectively. But multi-photon fluorescent image responds to the spatial distribution of multi-photon absorption coefficient. Therefore, SHG and THG confocal microscopy is a new imaging tool for living cell imaging, which can obtain new structural information of cells.

(3) The nonlinear effect of SHG and THG can sharpen the focal spot of SHG and THG, thus, the focal spots of SHG and THG are smaller than that of excitation light. The smaller the focal spot, the higher the resolution. Thus SHG and THG confocal microscopy can break through the resolution limit of Rayleigh's criterion and realize super-resolution imaging.

Acknowledgements This work was supported by the Team Project of the Natural Science Foundation of Guangdong Province (Grant No. 05012) and the National Major Fundamental Research Project of China (Grant No. 2002CCC00400).

References

1. Guo, Y., Ho, P. P., Savage, H. et al., Second-harmonic tomography of tissue, Opt. Lett., 1997, 22(17): 1323—1325.
2. Gauderon, U., Lukins, P. B., Sheppard, C. J. R., Three-dimensional second-harmonic generation imaging with femtosecond laser pulse, Opt. Lett., 1998, 23:1209—1211.
3. Dadap, J. I., Shan, J., Eisenthal, K. B. et al., Second-harmonic Rayleigh scattering from a sphere of centrosymmetric material, Phys. Rev. Lett., 1999, 83: 4045—4048.
4. Chu Shiwei, Chen Ihsiu, Liu Tzuming et al., Multimodal nonlinear spectral microscopy based on a femtosecond Cr:forsterite laser, Opt. Lett., 2001, 26(23): 1909—1911.
5. Paul, J. C., Andrew, C. M., Mark, T. et al., Three-dimensional high-resolution second-harmonic generation imaging of endogenous structural proteins in biological tissue, Biophys. J., 2002, 81(1): 493—508.
6. Verbiest, T., Elshocht, S. V., Kauranen, M. et al., Strong enhancement of nonlinear optical properties through supramolecular chirality, Science, 1998, 282: 913—915.
7. Denk, W., Strickler, J. H., Webb, W. W., Two-photon laser scanning fluorescence microscopy, Science, 1990, 248(6): 73—76.
8. Cumpstem, B. H., Ananthavel, S. P., Barlow, S. et al., Two-photon polymerization initiators for three-dimensional optical data storage and microfabrication, Nature, 1999, 398(4): 51—54.
9. Bewersdorf, J., Pick, R., Hell, S. W., Multifocal multiphoton microscopy, Opt. Lett., 1998, 23(9): 655—657.
10. Deitche, J., Kempe, M., Rudolph, W., Resolution in nonlinear laser scanning microscopy, J. Microscopy, 1994, 174(2): 69—73.
11. Gu Min, Sheppard, C. J. R., Optical transfer function analysis for two-photon 4Pi confocal fluorescence microscopy, Opt. Comm., 1995, 114: 45—49.
12. Tang Zhilie, Yang Chuping, Pei Hongjin et al., Imaging theory and resolution improvement of two-photon confocal microscopy, Science in China, Ser. A, 2002, 45(11): 1468—1478.
13. Goodman, J. W., Introduction to Fourier Optics, New York: McGraw-Hill, 1968.
14. Shen, Y. R., The Principles of Nonlinear Optics, New York: John Wiley & Sons, Inc., 1984.